JOURNAL OF GEOPHYSICAL RESEARCH, VOL. 108, NO. D13, 8504, doi:10.1029/2002JD002361, 2003

Vertical profiles of light scattering, light absorption, and single scattering albedo during the dry, biomass burning season in southern Africa and comparisons of in situ and remote sensing measurements of aerosol optical depths

Brian I. Magi and Peter V. Hobbs
Department of Atmospheric Sciences, University of Washington, Seattle, Washington, USA

Beat Schmid and Jens Redemann
Bay Area Environmental Research Institute, Sonoma, California, USA

Received 22 March 2002; revised 18 June 2002; accepted 8 July 2002; published 19 June 2003.

[1] Airborne in situ measurements of vertical profiles of aerosol light scattering, light absorption, and single scattering albedo (ω_0) are presented for a number of locations in southern Africa during the dry, biomass burning season. Features of the profiles include haze layers, clean air slots, and marked decreases in light scattering in passing from the boundary layer into the free troposphere. Frequency distributions of ω_0 reflect the strong influence of smoke from biomass burning. For example, during a period when heavy smoke was advected into the region from the north, the mean value of ω_0 in the boundary layer was 0.81 ± 0.02 compared to 0.89 ± 0.03 prior to this intrusion. Comparisons of layer aerosol optical depths derived from the in situ measurements with those measured by a Sun photometer aboard the aircraft show excellent agreement. *INDEX TERMS:* 0305 Atmospheric Composition and Structure: Aerosols and particles (0345, 4801); 0345 Atmospheric Composition and Structure: Pollution—urban and regional (0305); 3307 Meteorology and Atmospheric Dynamics: Boundary layer processes; 3359 Meteorology and Atmospheric Dynamics: Radiative processes; *KEYWORDS:* aerosols, particles, optical properties of particles

Citation: Magi, B. I., P. V. Hobbs, B. Schmid, and J. Redemann, Vertical profiles of light scattering, light absorption, and single scattering albedo during the dry, biomass burning season in southern Africa and comparisons of in situ and remote sensing measurements of aerosol optical depths, *J. Geophys. Res.*, *108*(D13), 8504, doi:10.1029/2002JD002361, 2003.

1. Introduction

[2] There is considerable current interest in scattering and absorbing aerosols because of their effects on the disposition of solar radiation as it passes through the atmosphere, and therefore on the temperature of the Earth [*IPCC*, 2001]. In particular, it is of importance to obtain measurements of the aerosol single scattering albedo (i.e., the ratio of the light scattered by particles to the particle extinction coefficient) and aerosol optical depths (AOD) in various parts of the world. Measurements made aboard the University of Washington's (UW) Convair-580 research aircraft in the SAFARI 2000 field study provided such measurements for southern Africa during the dry, biomass burning season (August and September 2000).

[3] In this paper, we present airborne in situ measurements of vertical profiles of aerosol light scattering, light absorption, and single scattering albedos at various locations in southern Africa (Figure 1) and under different meteorological conditions. We discuss the frequency distribution of values of the single scattering albedo at various locations and times. Finally, we compare layer AOD derived from the in situ measurements with those measured by a Sun photometer aboard the aircraft.

0148-0227/03/2002JD002361$09.00

2. Instrumentation

[4] All of the measurements described in this paper were obtained aboard the UW Convair-580 research aircraft. A complete listing of the Convair-580 flights in SAFARI 2000, the sampling strategies, and all of the instruments aboard the aircraft, is given in Appendix A by P. V. Hobbs in the work of *Sinha et al.* [2003]. The airborne measurements used in the present study were obtained as the aircraft changed altitude over various locations in southern Africa (Figure 1), from just above ground level, through the boundary layer, and into the free troposphere. Brief descriptions of the instrument used here are given below.

[5] Aircraft altitude and location were determined from an onboard global positioning system. The altitude was accurate to within about 5 m. Since the rate of climb (or descent) of the aircraft was $\sim 2-5$ m s^{-1}, and the instruments in this study provided output every second, the vertical resolution of the measurements presented here is 5 m.

[6] The dry aerosol light scattering coefficient, σ_{spd}, was measured with two independent nephelometers. One neph-

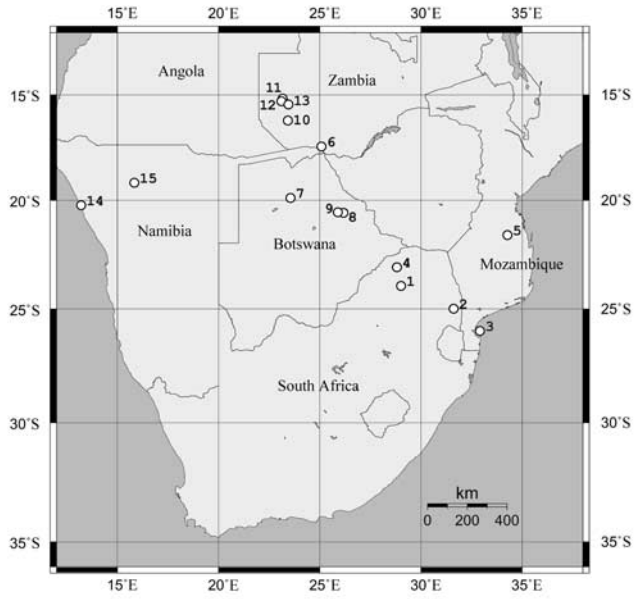

Figure 1. Locations of vertical profiles shown in this paper (circles). The number by each location is the case number given in the first column of Table 1.

elometer, custom-built for the UW by MS Electron and similar to the commercially available TSI nephelometer, provided simultaneous measurements of the light scattering coefficient and hemispheric backscatter coefficient at three visible wavelengths (450, 550, and 700 nm, with a nominal 40 nm bandwidth). The airstream to the MS nephelometer was heated to dry the aerosol and thereby eliminate the effects of ambient relative humidity (RH) on the measured aerosol light scattering and backscattering. *Hartley et al.* [2000] discuss details of the MS nephelometer, the precision of the measurements (~10%), and the methods used to correct the measurements for forward angular truncation and non-Lambertian illumination, which were used here. The other nephelometer (called the CE) measured the light scattering coefficient at 537 nm. The airstream to the CE nephelometer was not deliberately heated. However, since the ambient RH was generally low, and the aircraft cabin was warmer than the ambient air, the aerosol measured by the CE nephelometer was most likely dry. Measurements from the CE nephelometer are used here in only a few instances when MS nephelometer measurements were not available.

[7] To determine the effects of RH on light scattering by the aerosol, the aerosol light scattering coefficient was measured as a function of RH aboard the Convair-580 in SAFARI 2000, which provided so-called humidographs [*Magi and Hobbs*, 2003]. These measurements were used to adjust the light scattering measurements on the dried aerosol provided by the nephelometers to their corresponding values at the ambient RH.

[8] The dry aerosol light absorption coefficient, σ_{apd}, was measured at 567 nm (15 nm bandwidth) using a Particle and Soot Absorption Photometer (PSAP) described by *Hartley et al.* [2000]. The airstream to the PSAP was heated to dry the aerosol. The precision of the PSAP measurements is estimated to be ~25%. The PSAP provides 30 s running mean values of σ_{apd} with outputs every second. The PSAP measurements were converted to 550 nm by assuming an inverse wavelength dependence, as justified by *Hartley et al.* [2000] and *Bodhaine* [1995]. An internal flow meter in the PSAP monitors the flow rate at standard temperature and pressure (STP). Since the flow rate is needed to calculate σ_{apd}, it must be adjusted from STP to the ambient temperature and pressure. The values of σ_{apd} at ambient temperature and pressure were then corrected for errors in spot size, instrument-to-instrument variability, instrument noise, PSAP response to scattering, and PSAP response to absorption following the procedures described by *Bond et al.* [1999].

[9] The NASA 14-channel Ames Airborne Tracking Sun photometer (AATS-14) was mounted atop the UW Convair-580 aircraft. Provided that the solar disk was not obscured by cloud, the AATS-14 continuously recorded the total AOD above the altitude of the aircraft, which is referred to here as the "column AOD." The method of determining the column AOD from the Sun photometer measurements is described by *Schmid et al.* [2003].

3. Results and Discussion

3.1. Vertical Profiles of Light Scattering, Light Absorption, and Single Scattering Albedo

[10] Table 1 provides some basic information on all of the vertical profiles discussed in this paper, and Figure 1 shows the locations of the profiles.

[11] Shown in Figures 2–8 are seven examples of vertical profiles of the ambient aerosol light scattering coefficient at 550 nm, σ_{sp}, the dry aerosol light absorption coefficient at 550 nm (σ_{apd}), the single scattering albedo at 550 nm (ω_0), temperature and RH. Values of σ_{sp} were derived from the measured values of σ_{spd} and the appropriate humidographs as follows. *Magi and Hobbs* [2003] show that the following nonlinear equation provides an empirical fit to the humidograph data:

$$\sigma_{sp} = \sigma_{spd}\left[1 + a(RH/100)^b\right] \quad (1)$$

where a and b are fitting parameters. For cases 1–5 in Table 1, a = 2.55 ± 0.19, b = 3.59 ± 0.33; for cases 6–13 in Table 1, a = 1.44 ± 0.02, b = 4.88 ± 0.28; and for cases 14–15 in Table 1, a = 2.19 ± 0.32, b = 5.88 ± 0.57. These values of these fitting parameters are representative, respectively, of the ambient air in southern Africa during the period of our measurements (excluding a period of exceptionally heavy smoke), the ambient air during the exceptionally heavy smoke period, and the ambient air in Namibia [*Magi and Hobbs*, 2003]. Since all of the MS nephelometer measurements of σ_{spd} were made at about 30% RH, the corresponding value of σ_{sp} at RH is given by

$$\sigma_{sp}(RH) = \sigma_{spd}\left[\sigma_{sp}(RH)/\sigma_{sp}(30\%)\right] \quad (2)$$

[12] Humidographs were not available to derive values for the ambient absorption coefficient from the measured values of σ_{apd}. However, since the ambient RH was generally <50%, the measured values of σ_{apd} were probably close to the ambient absorption coefficient. The values of ω_0

Table 1. UW Convair-580 Flights in Southern Africa From Which Data Were Used in This Study[a]

Case Number	UW Flight Number	Date (2000)	Time Interval (hhmm UTC)	Mean Latitude (°S)	Mean Longitude (°E)	Minimum Aircraft Altitude (km msl)	Maximum Aircraft Altitude (km msl)	Layer AOD From Sun Photometer (τ_{sp})	Layer AOD From In Situ Measurements (τ_{is})
1	1819	20 Aug	1132–1146	23.95	29.01	1.71	3.77	0.09 ± 0.04	0.09 ± 0.01
2	1820	22 Aug	0816–1006	24.98	31.61	0.32	3.84	0.30 ± 0.04	0.25 ± 0.02
3	1822	24 Aug	0810–0824	25.98	32.91	0.16	4.15	0.23 ± 0.04	0.19 ± 0.01
4	1823	29 Aug	1030–1047	23.10	28.82	1.60	3.82	0.11 ± 0.05	0.10 ± 0.01
5	1825	31 Aug	1229–1244	21.62	34.27	0.57	3.89	0.24 ± 0.04	0.24 ± 0.01
6	1826	1 Sept	1051–1059	17.48	25.09	2.06	3.82	0.10 ± 0.05	0.13 ± 0.01
7	1829	2 Sept	0952–1009	19.89	23.55	1.04	4.47	0.29 ± 0.05	0.25 ± 0.02
8	1830	3 Sept	0831–0850	20.59	26.17	1.04	4.60	0.65 ± 0.05	0.59 ± 0.03
9	1830	3 Sept	1012–1035	20.56	25.90	0.95	4.58	0.55 ± 0.05	0.53 ± 0.03
10	1832	6 Sept	0746–0755	16.24	23.42	1.17	3.83	0.58 ± 0.05	0.64 ± 0.03
11	1832	6 Sept	0917–0929	15.19	23.16	1.32	4.77	0.82 ± 0.05	0.78 ± 0.05
12	1832	6 Sept	0934–0950	15.31	23.11	1.61	4.77	0.73 ± 0.06	0.72 ± 0.04
13	1832	6 Sept	0957–1014	15.47	23.46	1.61	5.32	0.83 ± 0.06	0.81 ± 0.05
14	1837	13 Sept	1116–1135	20.24	13.22	0.99	5.12	0.40 ± 0.05	0.32 ± 0.02
15	1839	16 Sept	1052–1107	19.19	15.84	1.28	4.77	0.19 ± 0.06	0.19 ± 0.01

[a]The values of the layer AOD derived from the Sun photometer (τ_{sp}) and in situ (τ_{is}) measurements are shown in the last two columns.

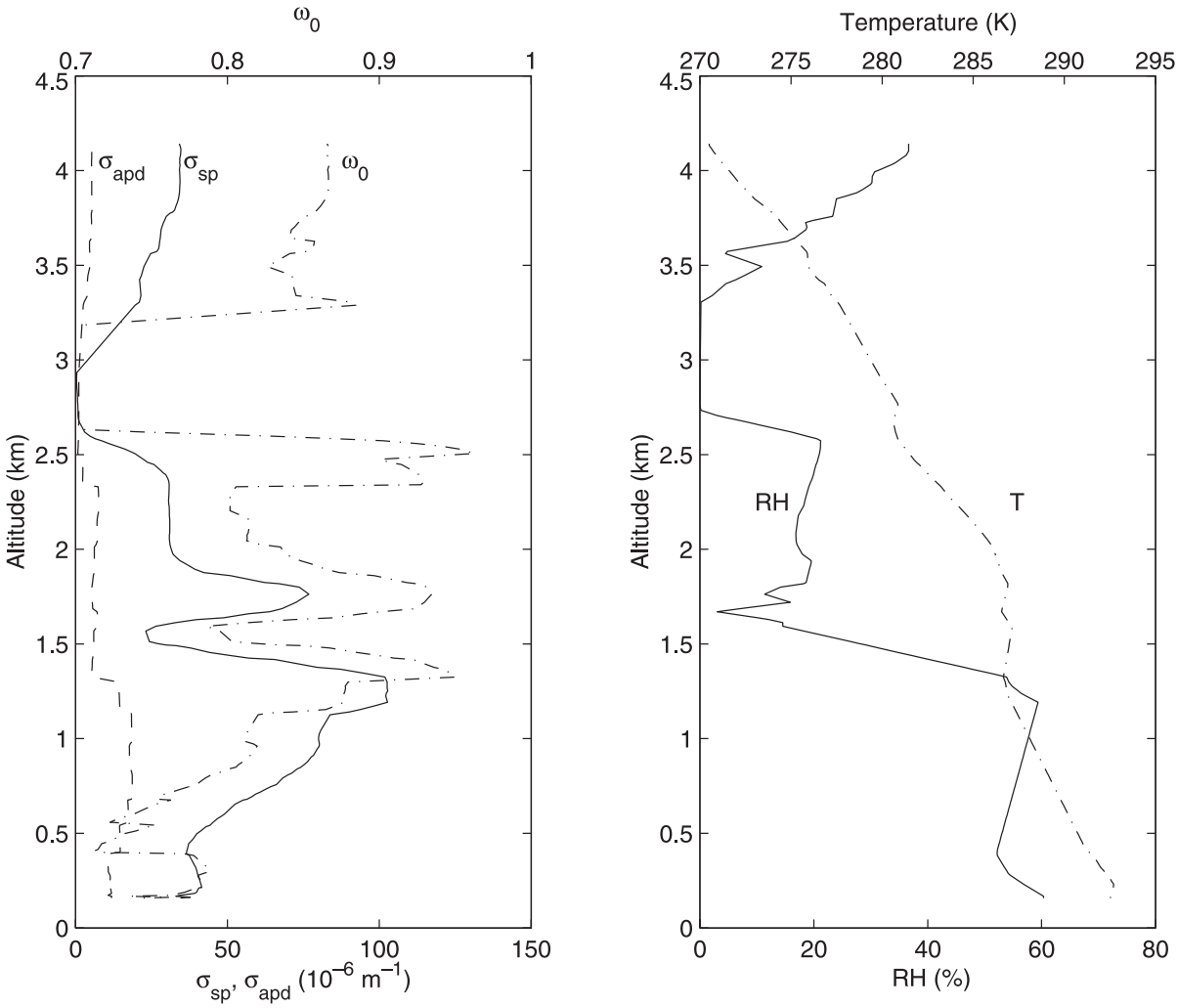

Figure 2. Vertical profiles from airborne in situ measurements of (a) the ambient aerosol light scattering coefficient (σ_{sp}), the dry aerosol light absorption coefficient (σ_{apd}), and the aerosol single scattering albedo (ω_0) at 550 nm and (b) the RH and temperature (T), over Inhaca Island, Mozambique from 0810 to 0824 UTC on 24 August 2000 (UW flight 1822). The lower end of the scale for $\bar{\omega}$ is terminated at 0.7 since values below this are subject to large errors. The vertical resolution of the measurements is 5 m.

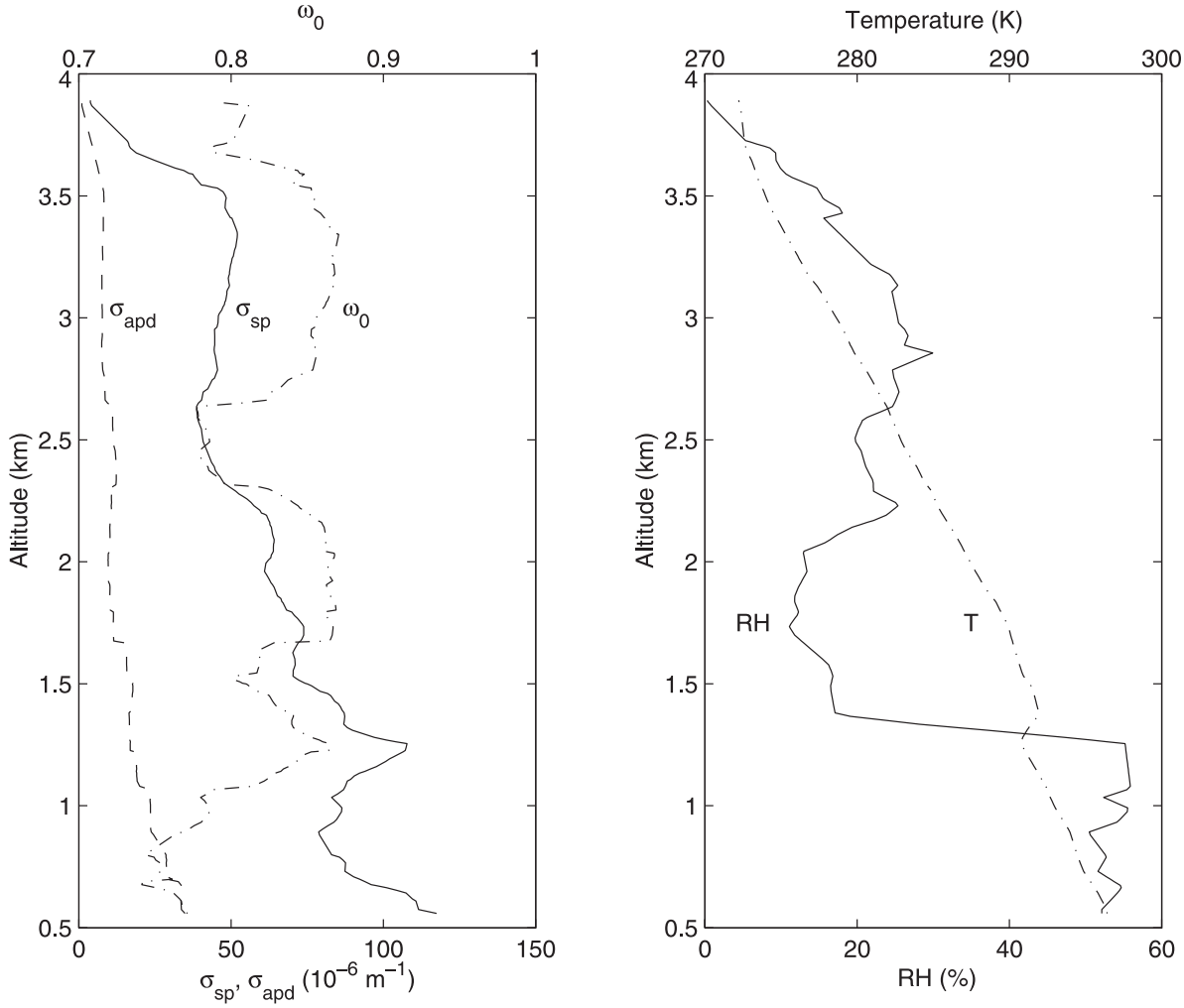

Figure 3. As for Figure 2 but over northeast Mozambique from 1229 to 1244 UTC on 31 August 2000 (UW flight 1825).

shown in Figures 2–8 are for a wavelength of 550 nm and were calculated from

$$\omega_0 = \frac{\sigma_{sp}}{\sigma_{sp} + \sigma_{apd}} \quad (3)$$

[13] The PSAP provided 30 s running means of σ_{apd} with outputs every second. Therefore, the nephelometer measurements of σ_{sp} were also averaged over running 30 s periods with outputs every second.

[14] The vertical profiles shown in Figure 2 were obtained on 24 August 2000, over Inhaca Island, Mozambique. Haze layers are evident in the light scattering profile at ~1.3 and ~1.75 km, and a clean air slot [*Hobbs*, 2002, 2003] is present from ~2.75 to 3.25 km. The single scattering albedo varies between ~0.7 and 1.0, indicating a variable distribution of smoke in the vertical. Values of ω_0 in the clean air slot could not be reliably calculated because the values of σ_{sp} and σ_{apd} were below their reliable detection limits.

[15] The profiles shown in Figure 3 were obtained on 31 August 2000, over the northeast coast of Mozambique, where the lower boundary layer (from about 0.6 to 1.4 km) was dominated by smoke from extensive localized biomass burning, as indicated by the higher values of σ_{sp} and σ_{apd} in that layer. Above this layer, and above the temperature inversion, is a layer with lower values of σ_{sp} and σ_{apd}, indicating that the smoke from the local biomass burning was trapped below the temperature inversion. A small increase in σ_{sp} between about 2.4 and 2.6 km was probably caused by an elevated layer of smoke. The sharp fall off in σ_{sp} and RH above about 3.5 km marks the base of the free troposphere. The values of ω_0 on 31 August are generally lower than on 24 August, indicating that the aerosol was more absorbing.

[16] The vertical profiles shown in Figure 4 were obtained over Maun, Botswana, between 0952 and 1009 on 2 September 2002. It can be seen from the profiles in Figure 4 that the aircraft entered the free troposphere at an altitude of ~4 km, where the values of σ_{sp}, σ_{apd}, and RH decreased sharply. Values of ω_0 were fairly uniform and low in the boundary layer, but increased rapidly at the top of the boundary layer prior to the readings from the MS nephelometer and PSAP dropping below their detection limits. The RH was also fairly uniform in the mixed layer, but decreased rapidly in the free troposphere.

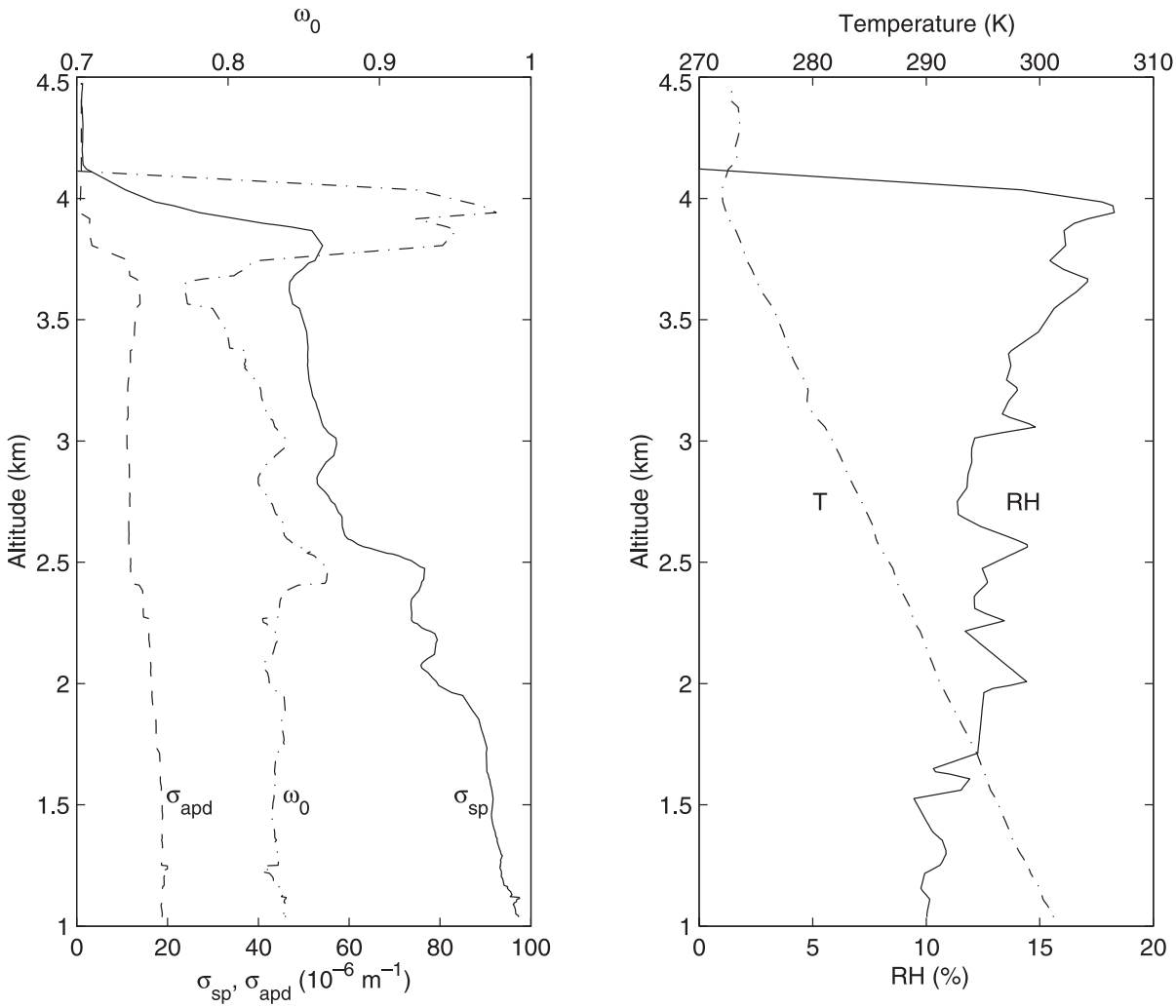

Figure 4. As for Figure 2 but over Maun, Botswana from 0952 to 1009 UTC on 2 September 2000 (UW flight 1829).

[17] The values of σ_{sp} and σ_{apd} in Figures 5–7, which were obtained over Botswana and Zambia during the period 3–6 September 2000, are notably larger than those in Figures 2–4. This is attributable to a shift in synoptic conditions, which caused smoke from extensive biomass burning in tropical southern Africa to be transported in a northwest-to-southeast channel from Zambia to southern Mozambique during the period 3–10 September 2000. This is the so-called River of Smoke described by *Swap et al.* [2003]. This unusually heavy smoke decreased visibility levels in the region of our measurements, and the elevated levels of absorbing carbon aerosol produced noticeable increases in σ_{apd}.

[18] Figure 5 (0831–0850 UTC on 3 September 2000) shows two distinct layers of elevated light scattering, one between ~1 and 1.6 km and the other between ~2 and 2.75 km, over the Sua Pan, Botswana. There is a clean air slot between these two haze layers, where the light scattering is similar to that above 2.75 km. The values of σ_{apd} are fairly uniform above 2.75 km, but are higher in the two haze layers.

[19] Figure 6 shows vertical profiles obtained over the same general location as those shown in Figure 5 but about 1-1/2 hours later. The light scattering coefficients were still high, and the single scattering albedos low, but by this time the clean air slot had disappeared. The values of σ_{sp} and σ_{apd} generally decreased with height, resulting in ω_0 values that oscillated around 0.8.

[20] Figure 7 shows profiles over Mongu, Zambia on 6 September 2002, which is in the heart of the "River of Smoke" in terms of both location and time. The values of σ_{sp} and σ_{apd} are uniformly high, with some evidence of haze layer structuring. One feature of the profile is the height of the mixed boundary layer, which extended above 5 km, and nearly reached the 500 hPa pressure level (not shown). The light scattering values at altitudes >5 km were greater than anything we measured in August 2000 (see, for example, Figures 2 and 3). The lack of strong temperature inversions on 6 September no doubt contributed to the mixing of the smoke to altitudes >5 km as it was transported over long distances from the north.

[21] The profiles shown in Figure 8 were obtained above a marine stratocumulus cloud deck off the Namibia coast on 13 September 2000. Parcel back trajectories (obtained using the software provided by NOAA: http://www.arl.noaa.gov/ready/hysplit4.html) show that from ~1.2 to 2.4 km the

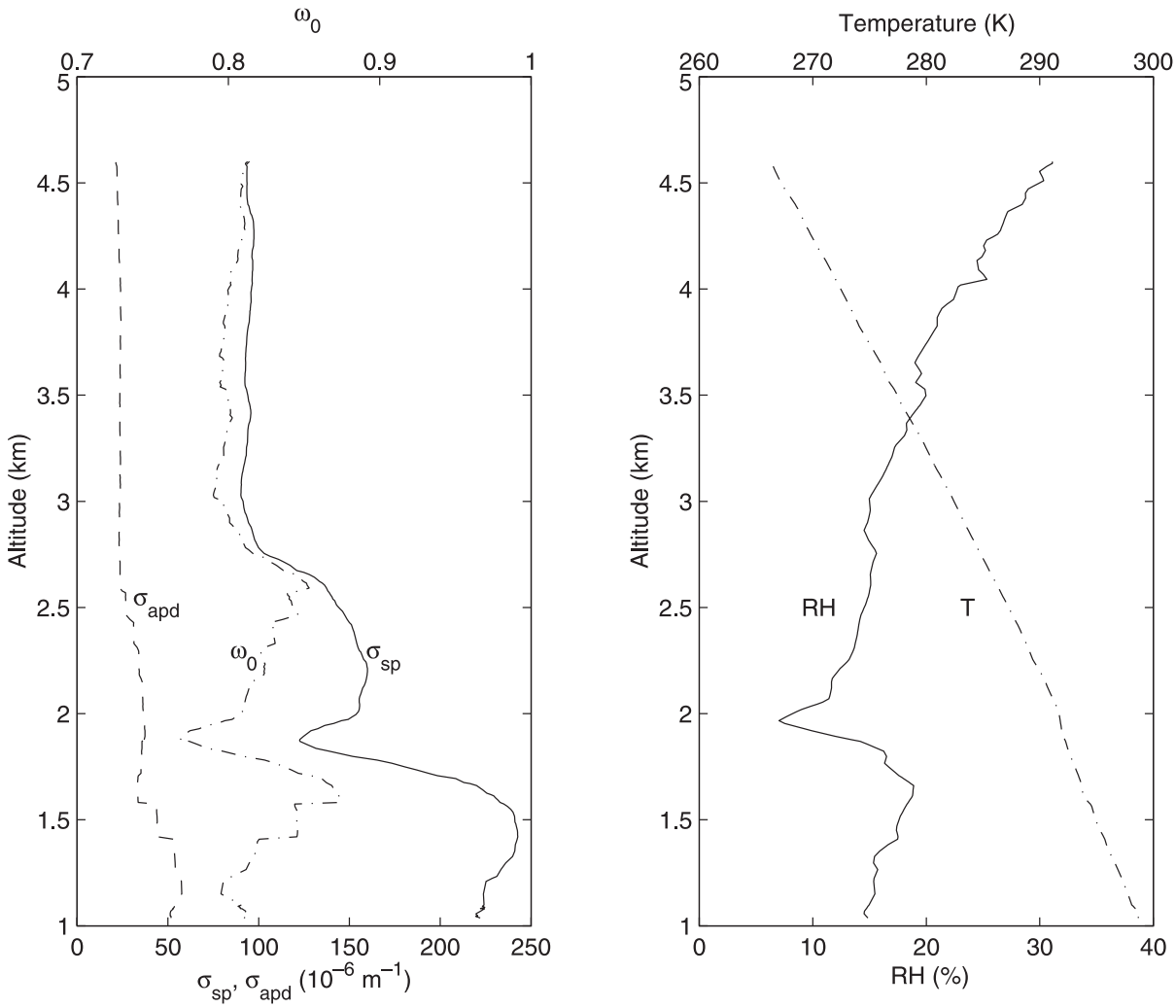

Figure 5. As for Figure 2 but over the Sua Pan, Botswana from 0831 to 0850 UTC on 3 September 2000 (UW flight 1830).

airflow was onshore; in this region σ_{sp} is low and ω_0 relatively high. Above ~2.4 km, there was continental outflow, presumably containing biomass smoke, which produced high light scattering and low single scattering albedos.

3.2. Frequency Distributions of the Single Scattering Albedo in the Mixed Boundary Layer

[22] Scattering by aerosols will tend to keep a layer of air cool, whereas, absorption by aerosols will warm the layer. Therefore, ω_0 is a key parameter in determining whether a layer is cooled or heated. Whether absorption by aerosols increases or decreases the amount of radiation returned to space depends on both ω_0 and the reflectivity of the underlying surface. For example, for savanna with a surface reflectivity of 10%, values of ω_0 less than about 0.4 are predicted to cause warming [e.g., *Seinfeld and Pandis*, 1998].

[23] The vertical profiles of ω_0 are shown in Figures 2–8. These values were obtained primarily in the mixed boundary layer but, on occasions the aircraft entered the free troposphere (e.g., above about ~3.5 and 4 km in Figures 3 and 4, respectively) and also clean air slots [*Hobbs*, 2002, 2003; *Sinha et al.*, 2003, Appendix A] sandwiched between layers of elevated haze (e.g., between ~2.5 and 3 km in Figure 2 and just below 2 km in Figure 5). The values of ω_0 obtained in the mixed boundary layer for cases 1–13 in Table 1 were categorized as either (1) regional aerosol exemplifying the typical background aerosol during the dry season, in southern Africa or (2) regional aerosol perturbed by intrusions of heavy smoke. Quantitatively, we found that those portions of a vertical profile with $\sigma_{apd} > 11 \times 10^{-6}$ m^{-1} (i.e., with relatively high carbon content) indicated the presence of heavy smoke and thus fell into category 2. The values of ω_0 obtained in Namibia (cases 14–15 in Table 1) are considered separately for reasons discussed below.

[24] In this section, we present frequency distributions for values of ω_0 obtained in the mixed boundary layer for all the cases listed in Table 1, but excluding clean air slots and measurements made in the free troposphere (where values of ω_0 derived from σ_{sp} and σ_{apd} are generally unreliable due to lack of sensitivity of the MS nephelometer and the PSAP measurements in clean air).

[25] Figure 9 shows four frequency distribution plots for ω_0. Figure 9a are ω_0 values for category 1 defined above. Generally, cases 1–5 in Table 1 fell into this category, except when localized heavy smoke was encountered. For

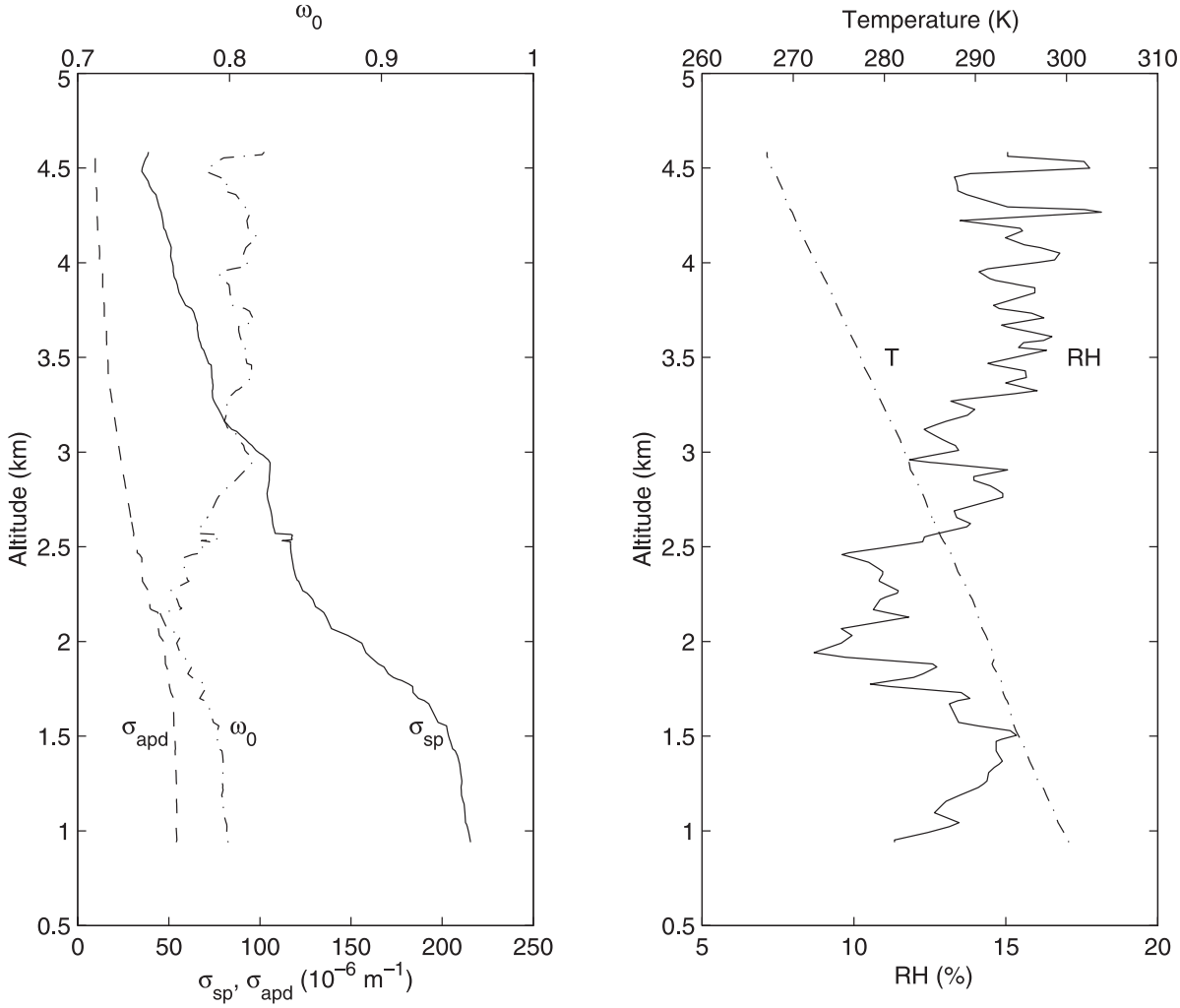

Figure 6. As for Figure 2 but over the Sua Pan, Botswana from 1012 to 1035 UTC on 3 September 2000 (UW flight 1830).

example, the vertical profile obtained in Mozambique (Figure 3) has a clear contribution from heavy smoke in the 0.6–1.4 km layer, which derived from extensive localized biomass burning. Therefore, values of ω_0 in this layer were assigned to category 2. The mean value of ω_0 for category 1 was 0.89 ± 0.03, with a few values near 0.8 and some values above 0.98 (Figure 9a).

[26] Figure 9b shows ω_0 values for category 2 defined above. Cases 6–13 in Table 1 generally fell into this category. Vertical profiles 6 and 7 in Table 1 were obtained during a regional transition period, just prior to the "River of Smoke" episode, but some locales (e.g., southern Zambia and northern Botswana) were already affected by the heavy smoke from the north. This is evident in the elevated σ_{apd} values, which generally exceed by 2–3 times the σ_{apd} values for cases 1–5 in Table 1. Cases 8–13 in Table 1 were obtained during the "River of Smoke"; they exhibit greater light absorption and light scattering due to heavy smoke at all altitudes up to ~4.5 km. This is reflected in the mean value of ω_0 for category 2, which was 0.81 ± 0.02, indicating more absorbing aerosols with higher black carbon content.

[27] The frequency distribution of $\bar{\omega}$ shown in Figure 9c is based on measurements obtained on 13 September in a flight just off the Namibian coast (case 14 in Figure 1 and Table 1, see also Figure 8). As discussed in section 3.1, below ~2.4 km the airflow was from the west and relatively clean, but above this height there was continental outflow. This produced two distinct distributions of ω_0, which are reflected in the bimodal frequency distribution shown in Figure 9c. We attribute the modal distribution of ω_0 that peaks at values just above 0.80 in Figure 9c to the long-range transport of biomass smoke to Namibia from north and east, where biomass burning is common. This interpretation is supported by the fact that carbon monoxide concentrations increased by a factor of ~3, ozone concentrations by a factor of ~1.8, and the condensation nucleus concentrations by a factor of ~4, when the aircraft climbed above ~2.4 km. Prior to the "River of Smoke" episode, the ratio of sulfate mass to total particulate mass in the interior of southern Africa was ~20–40%. During the "River of Smoke" episode, this ratio decreased to 4–8%. The corresponding ratio was ~7% at an altitude of 3.6 km off the Namibian coast on 13 September. This also supports the view that the air above ~2.4 km off the Namibian coast on 13 September was dominated by smoke.

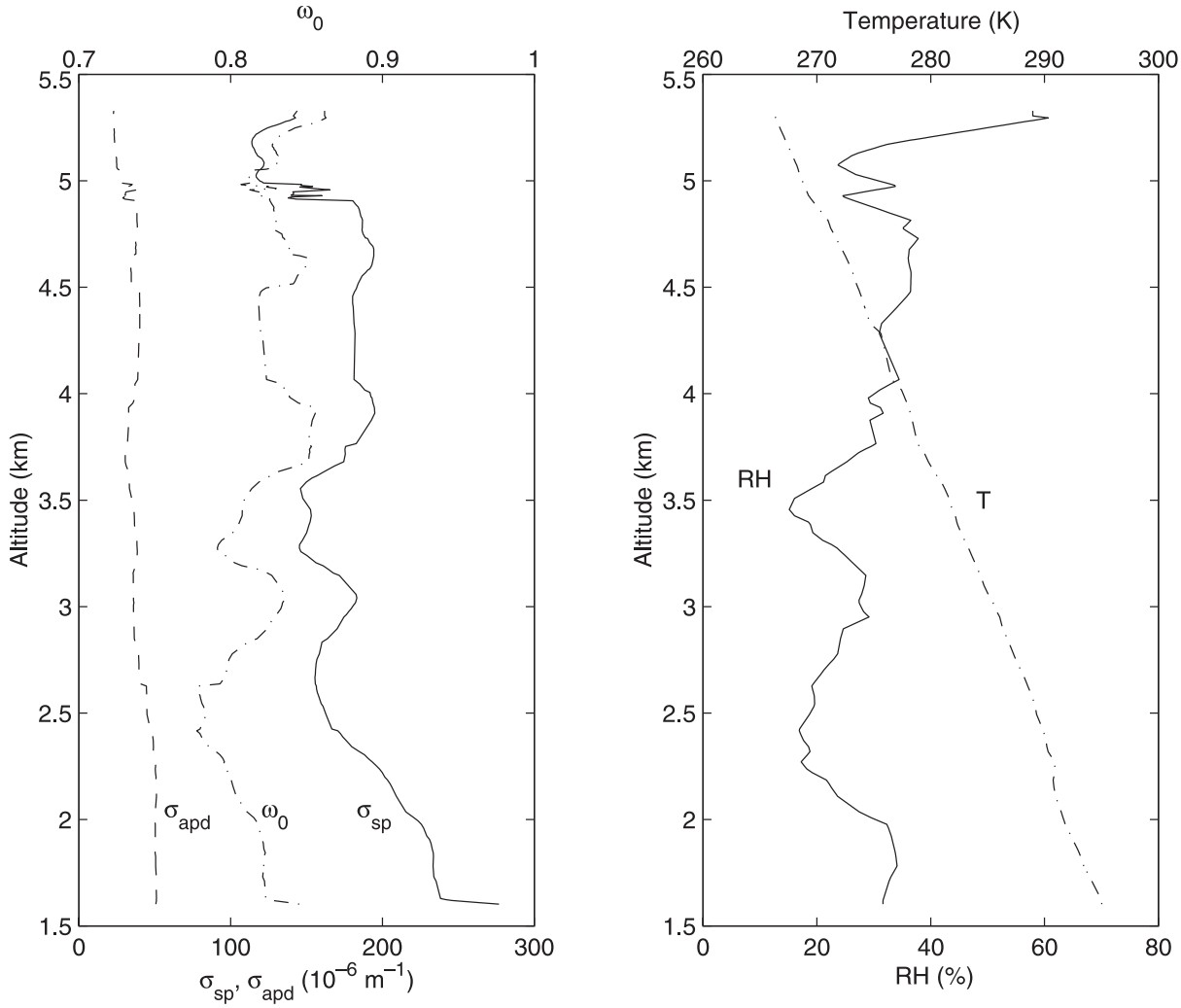

Figure 7. As for Figure 2 but over Mongu, Zambia from 0957 to 1014 UTC on 6 September 2000 (UW flight 1832).

[28] Figure 9d shows the frequency distributions of ω_0 from measurements obtained on 16 September over the Etosha Pan in Namibia (case 15 in Figure 1 and Table 1). Here the mean value of ω_0 is relatively large (0.90 ± 0.05), and the most common value of ω_0 is 0.94. Back trajectories for this case show the air sampled over the Etosha Pan came from southwestern Botswana and northern South Africa, but there was no evidence for smoke over the Etosha Pan.

3.3. Comparison of Airborne Sun Photometer and In Situ Measurements of AOD

[29] The airborne Sun photometer provided remote sensing measurements of the column AOD. In a rapid tight spiral climb or descent of the aircraft, the difference in column AOD between any two altitudes measured by the Sun photometer provides the AOD between those two points, which we call the "layer AOD." We will refer to layer AOD measured by the Sun photometer as τ_{sp}.

[30] The layer AOD between heights z_1 and z_2 ($z_1 < z_2$) is given by

$$\tau = \int_{z_1}^{z_2} \sigma_{ep}(z)dz \qquad (4)$$

where $\sigma_{ep}(z)$ is the ambient aerosol light extinction coefficient at height z, and

$$\sigma_{ep}(z) = \sigma_{sp}(z) + \sigma_{ap}(z) \qquad (5)$$

where, $\sigma_{sp}(z)$ and $\sigma_{ap}(z)$ are the ambient aerosol light scattering coefficient and the ambient aerosol light absorption coefficient at altitude z, respectively. The light scattering and light absorption coefficients for the dried aerosol were measured by the nephelometers and PSAP, respectively, aboard the Convair-580 aircraft. However, before these values can be used in (5) and then in (4) to compute a layer AOD from the in situ measurements for comparison with the ambient AOD measured by the Sun photometer, they should be multiplied by appropriate hygroscopic growth factors for light scattering and light absorption using the empirical approach described in section 3.1. Hence, the ambient AOD between heights z_1 and z_2 from the in situ measurements is given by

$$\tau_{is} = \int_{z_1}^{z_2} \left(\sigma_{spd}\, f_s + \sigma_{apd}\, f_a\right)dz \qquad (6)$$

where, $\sigma_{spd}(z)$ is the dry aerosol light scattering coefficient, $\sigma_{apd}(z)$ the dry aerosol light absorption coefficient, and f_s

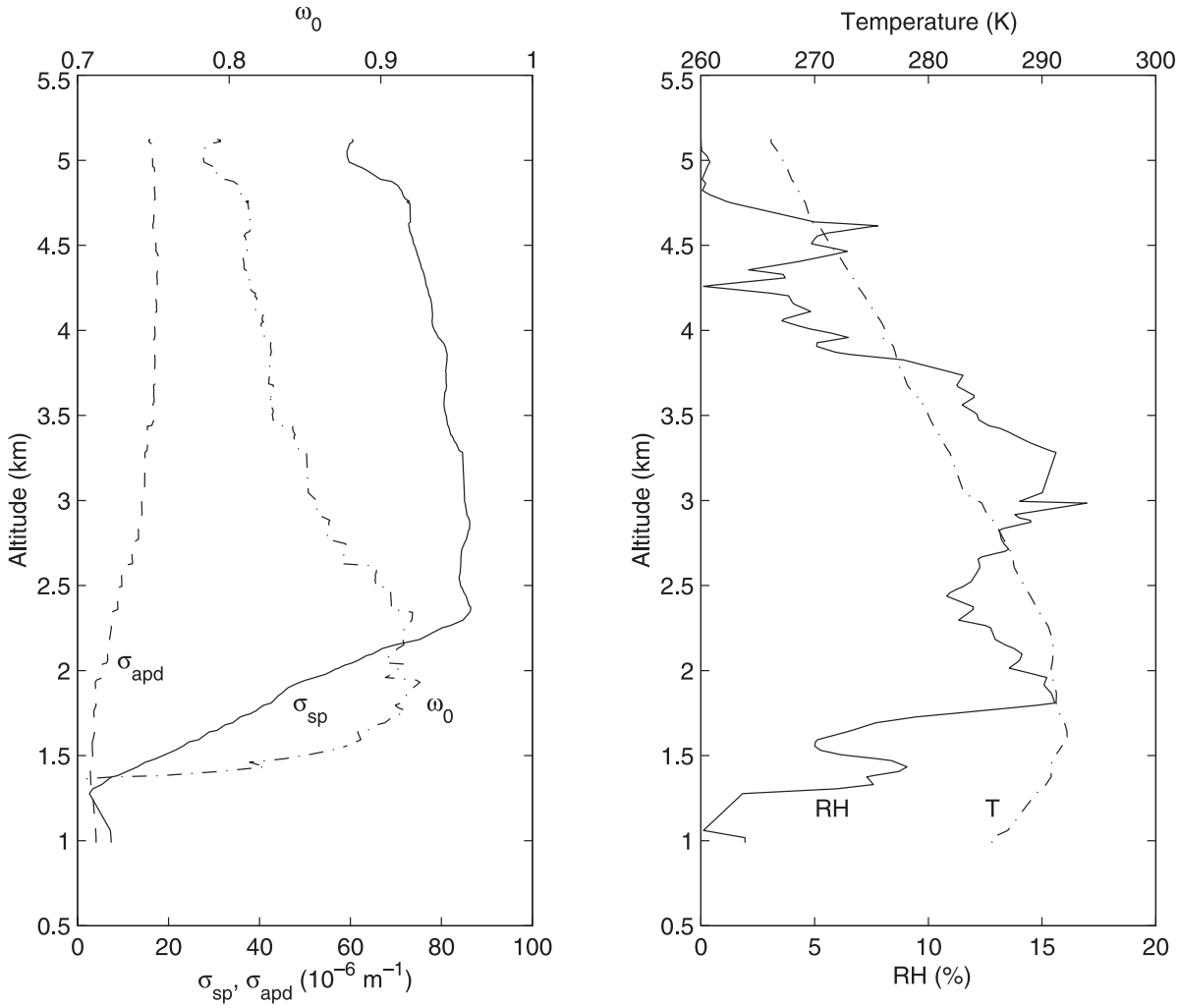

Figure 8. As for Figure 2 but off coast of Namibia from 1116 to 1135 UTC on 13 September 2000 (UW flight 1837).

and f_a are the empirical growth factors by which the scattering and absorption coefficients, respectively, must be multiplied to adjust their values to the ambient RH. As described in sections 2 and 3.1, σ_{spd} and σ_{apd} were measured, and f_s was determined from humidographs [*Magi and Hobbs*, 2003]. However, f_a was not measured. The value of f_a must lie between 1 and f_s [*Hegg et al.*, 1997; *Redemann et al.*, 2001]. Since the ambient RH in this study was generally <50%, and $\sigma_{apd} \ll \sigma_{spd}$, we assume here (as did Hegg et al.) that $f_a = 1$.

[31] Calculation of τ_{is} from (6) requires continuous measurements of σ_{spd}, σ_{apd} between z_1 and z_2. With the exception of UW flight 1832, 0917–0929 UTC and 0957–1014 UTC, these measurements were provided by the MS nephelometer and PSAP, respectively. For the two exceptions, the σ_{spd} values at 550 nm were estimated from the CE nephelometer measurements at 537 nm. *Magi and Hobbs* [2003] show that the RH dependence of f_s changed significantly during SAFARI 2000, particularly during the period 3–10 September when the "River of Smoke" occurred. These variations in f_s were taken into account in evaluating τ_{is} from (6). Also, in general, f_s might be expected to vary with altitude (z). However, our measurements in SAFARI 2000 showed that up to an altitude of 4 km at least, the altitude dependence of f_s was minimal [*Magi and Hobbs*, 2003].

[32] In comparing τ_{sp} with τ_{is} a common wavelength must be used. All AOD values reported in this study are for a wavelength of 550 nm. The MS nephelometer provides measurements of σ_{spd} at 550 nm. The PSAP provides measurements of σ_{apd} at 567 nm; these values were adjusted to 550 nm using the method described in section 2. The AATS-14 Sun photometer provided the AOD at 14 discrete wavelengths from 354 to 1558 nm. To derive the AOD at 550 nm from the AATS-14 measurements, the quadratic polynomial interpolation equation given by *Schmid et al.* [2003] was used.

[33] The column AOD above height z_1 measured by the Sun photometer can be compared with the in situ measurements by adding the column AOD measured by the Sun photometer at height z_2 to τ_{is} evaluated between z_1 and z_2. The comparison of column AOD values for seven cases (corresponding to the seven cases shown in Figures 2–8) are shown in Figures 10–16, respectively, the column AOD measured by the Sun photometer should decrease monotonically with increasing altitude. However, this was not

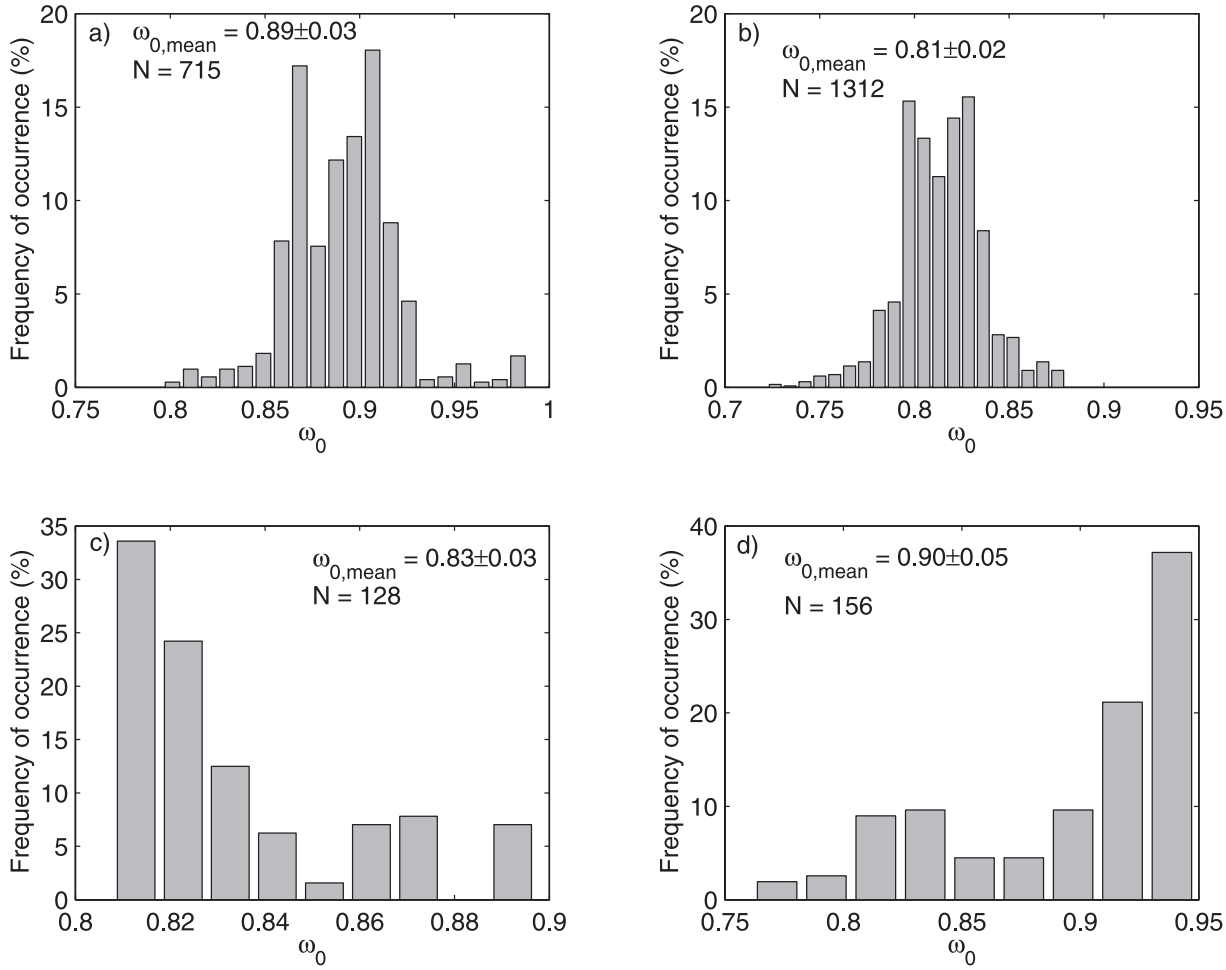

Figure 9. Frequency distributions of the ambient single scattering albedo (ω_0) at 550 nm in the boundary layer derived from in situ measurements obtained at the locations shown in Figure 1 and listed in Table 1. The mean value of ω_0 and standard deviation of ω_0 are shown for each distribution. N is the total number of data points in each distribution. (a) Regional aerosol exemplifying the typical background aerosol in southern Africa (generally cases 1–5 in Table 1 from 20 to 31 August 2000). (b) Regional aerosol perturbed by heavy smoke from either local sources or long-range transport during the "River of Smoke" episode (generally cases 6–13 in Table 1 from 1 to 6 September 2000). (c) Case 14 on 13 September 2000 near the coast of Namibia. (d) Case 15 in Table 1 on 16 September 2000 over the Etosha Pan in the northern interior of Namibia.

always the case in practice because of temporal fluctuations and spatial inhomogeneities in the atmosphere during the period required to obtain the measurements that comprise a vertical profile.

[34] The layer AOD derived from the Sun photometer and calculated from the in situ measurements are listed in the last two columns of Table 1. Various layer AOD closure studies have been reported previously. *Hegg et al.* [1997] and *Hartley et al.* [2000] used measurement from a Sun photometer mounted on an aircraft and in situ nephelometer and PSAP measurements from the same aircraft, obtained on flights off the U.S. East Coast. The comparisons were in good agreement. On the other hand, *Remer et al.* [1997] and *Kato et al.* [2000] compared ground-based measurements of AOD with values derived from airborne in situ measurements and did not obtain good agreement. *Schmid et al.* [2000] compared AOD measurements from airborne AATS-14 instrument with those derived from nephelometer and PSAP measurements aboard the same aircraft flying in air masses dominated by marine and dust aerosols. They also did not obtain agreement between the two data sets, probably because particles were sampled through an inlet that was inadequate for sampling the large particles typical of marine and dusty air.

[35] Figure 17 shows the results from the present study using all of the layer AOD derived from the Sun photometer (τ_{sp}) and those calculated from the in situ measurements (τ_{is}). The best-fit straight line to τ_{is} versus τ_{sp} lies close to the perfect-fit (1 to 1) line ($r^2 = 0.98$). The empirical best-fit line relating the two data sets is

$$\tau_{is} = (0.96 \pm 0.06)\tau_{sp} - (0.007 \pm 0.034) \quad (7)$$

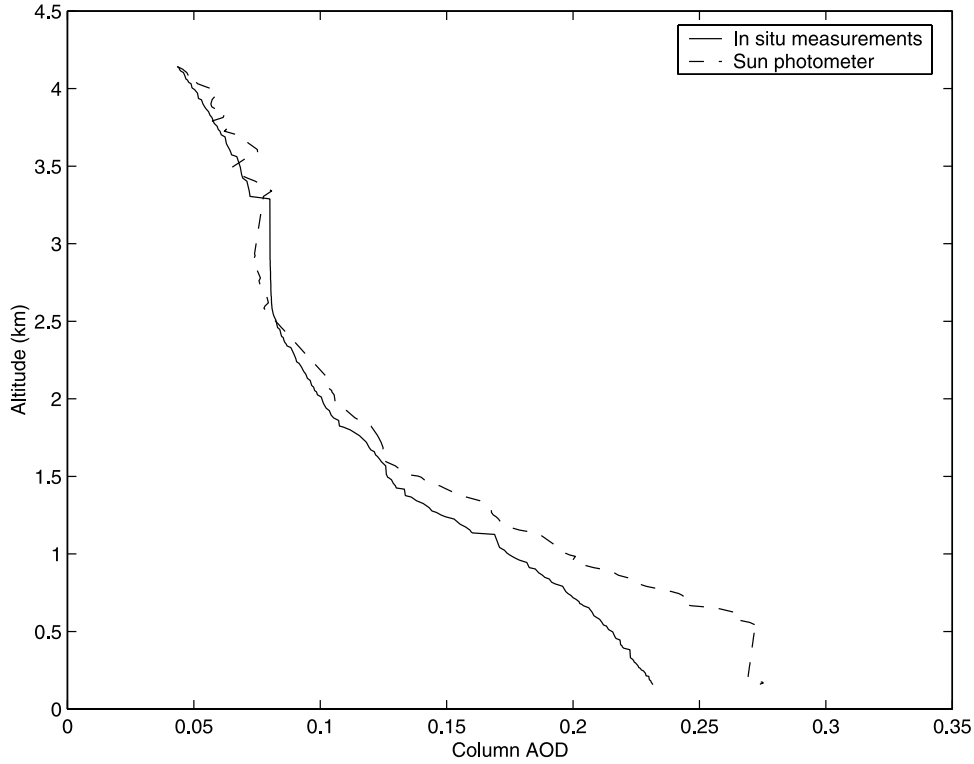

Figure 10. Comparison of column AODs at 550 nm derived from the airborne Sun photometer (dashed line) and the in situ measurements (solid line) over Inhaca Island, Mozambique from 0810 to 0824 UTC on 24 August 2000 (UW flight 1822).

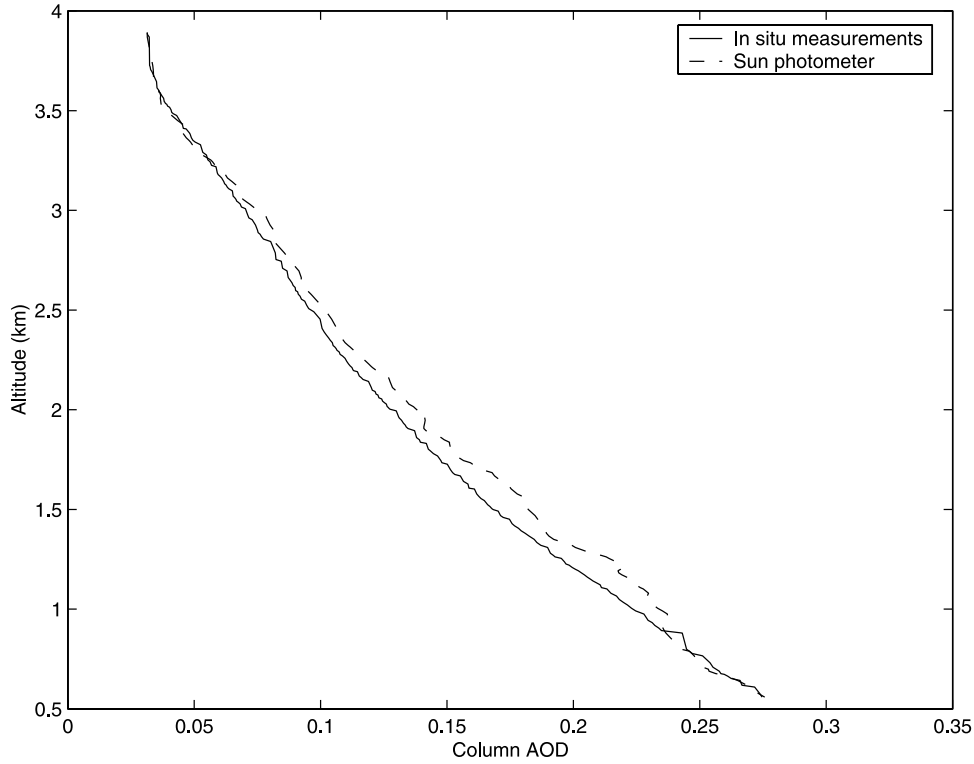

Figure 11. As for Figure 10 but over northeast Mozambique from 1229 to 1244 UTC on 31 August 2000 (UW flight 1825).

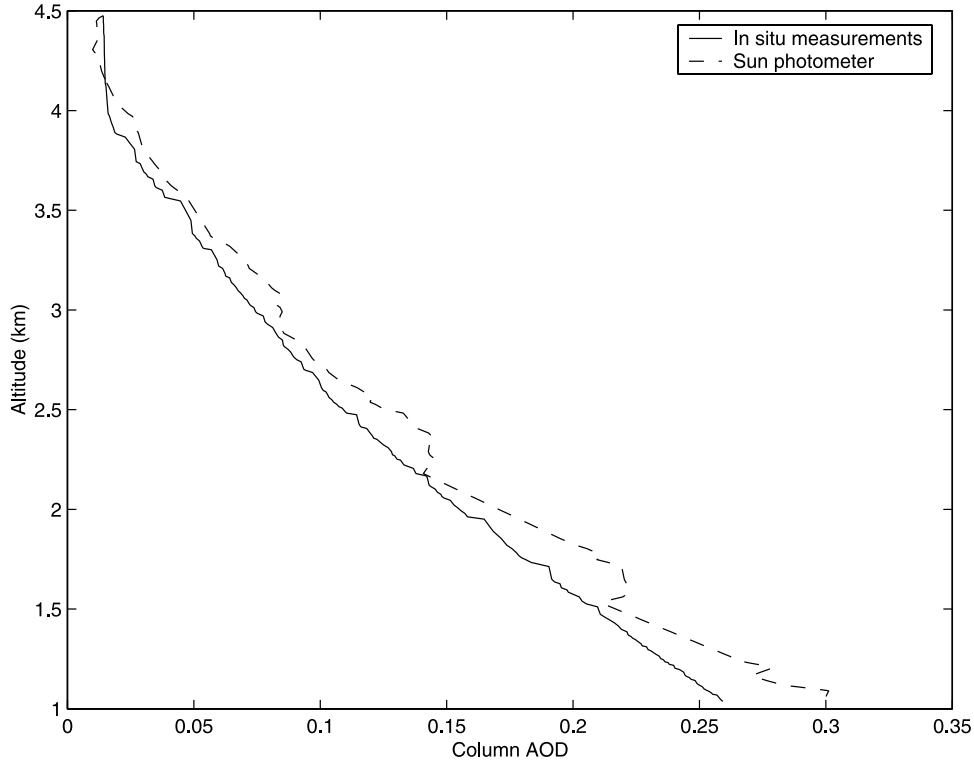

Figure 12. As for Figure 10 but over Maun, Botswana from 0952 to 1009 UTC on 2 September 2000 (UW flight 1829).

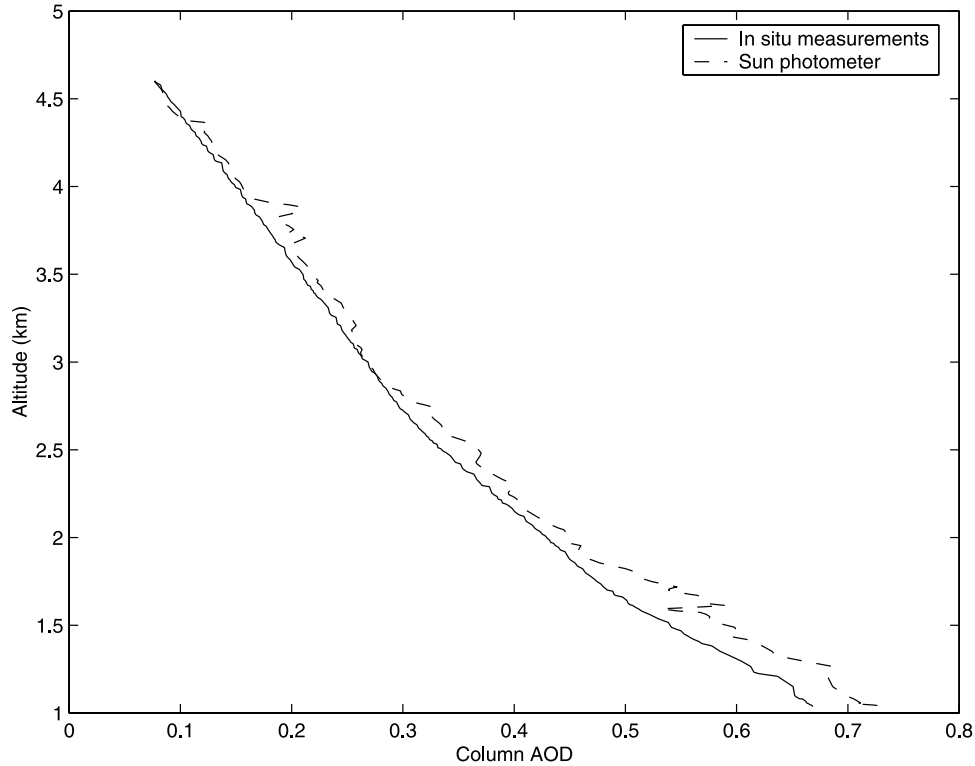

Figure 13. As for Figure 10 but over the Sua Pan, Botswana from 0831 to 0850 UTC on 3 September 2000 (UW flight 1830).

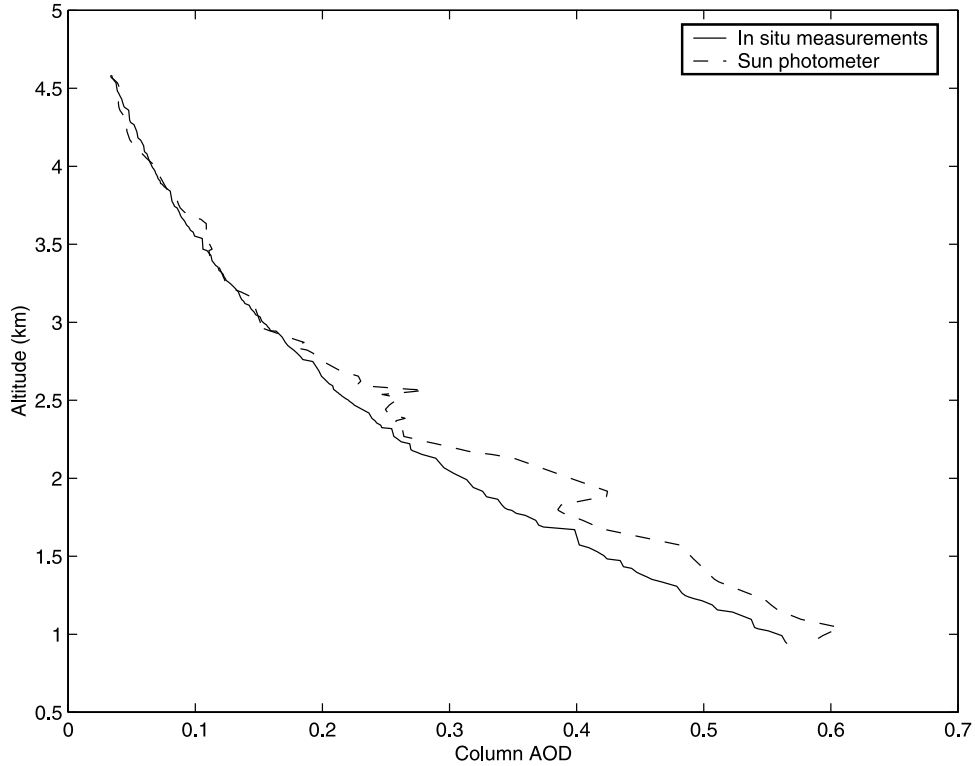

Figure 14. As for Figure 10 but over the Sua Pan, Botswana from 1012 to 1035 UTC on 3 September 2000 (UW flight 1830).

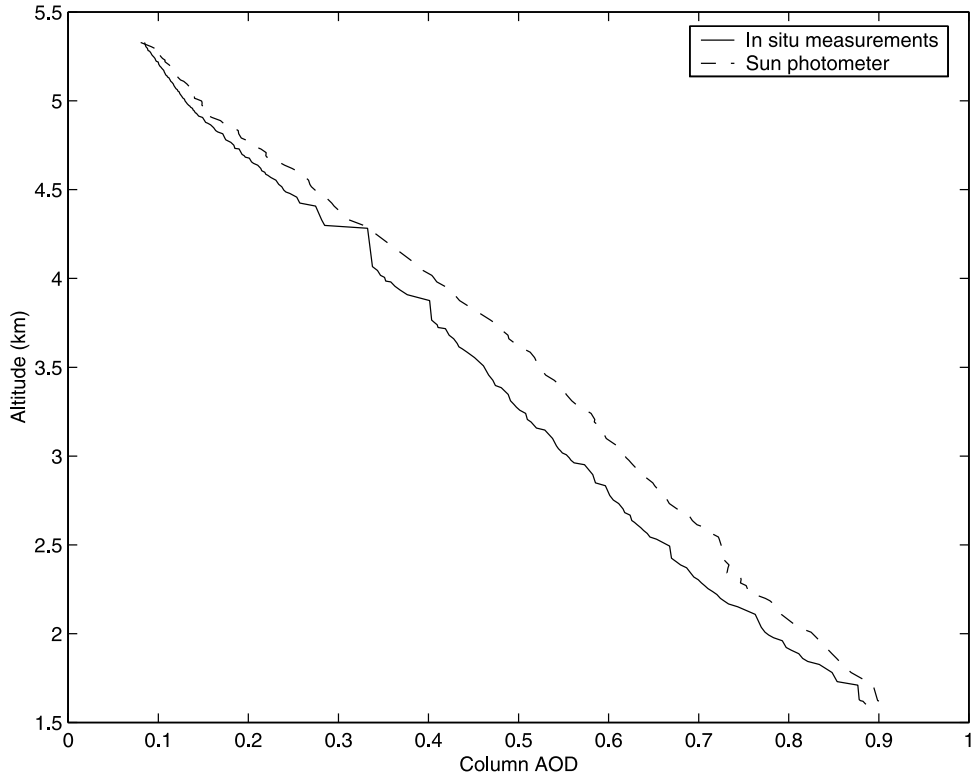

Figure 15. As for Figure 10 but over Mongu, Zambia from 0957 to 1014 UTC on 6 September 2000 UTC (UW flight 1832).

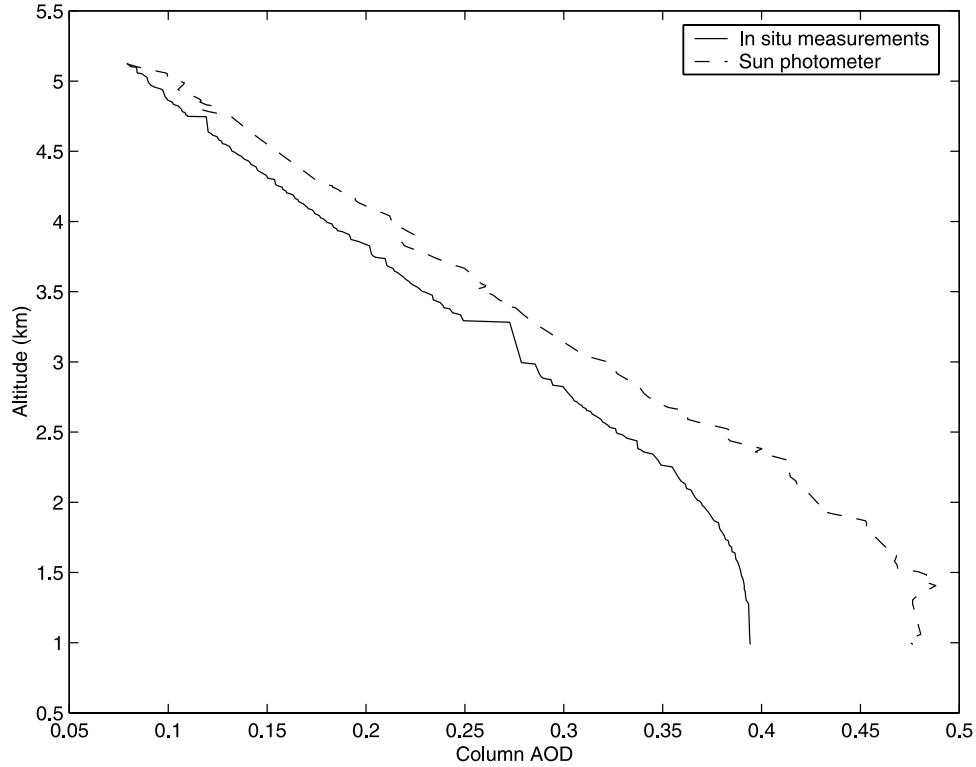

Figure 16. As for Figure 10 but off the coast of Namibia from 1116 to 1135 UCT on 13 September 2000 (UW flight 1837).

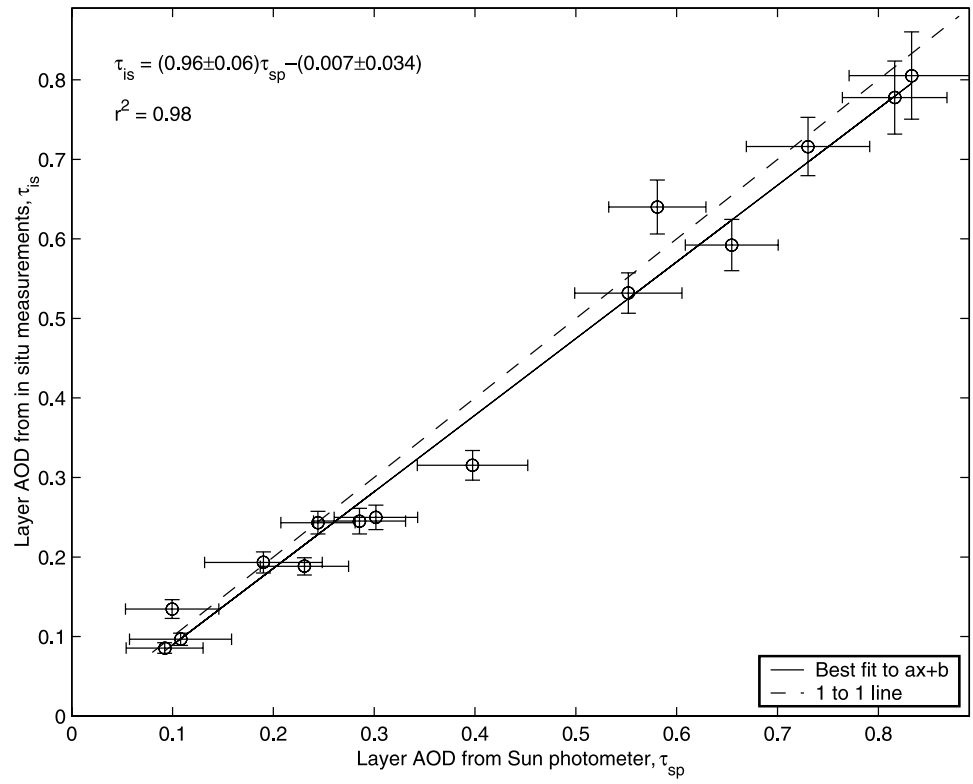

Figure 17. Comparison of layer AODs at a wavelength of 550 nm derived from airborne Sun photometer and in situ measurements. The best-fit straight line to the data points is shown by the solid line. The 1-to-1 perfect correlation is shown by the dashed line.

Thus, the AOD derived from the Sun photometer and the in situ measurements were, in general, in excellent agreement.

[36] The best closure results predating this study are those of *Hegg et al.* [1997] and *Hartley et al.* [2000], which were based on the same data covering 12 profiles flown mostly in the marine boundary layer off the U.S. East Coast. Their best-fit straight line to τ_{is} versus τ_{sp} resulted in a slope of 0.86 with $r^2 = 0.90$. Our slope of 0.96 and $r^2 = 0.98$ makes it the most successful closure study to date.

[37] *Schmid et al.* [2003] noted that in virtually all previous closure studies, the in situ measurements yielded lower values than those obtained from Sun photometer measurements. They suggested the following might account for these differences: (1) possible loss of semivolatile aerosol material during direct sampling [*Eatough et al.*, 1996] and (2) gas absorption that may be present in the atmosphere, which is not accounted for in Sun photometer analyses [e.g., *Halthore et al.*, 1998]. The present study suggests that (2) can be ruled out and that (1) seems to play a minor role for the aerosol sampled in SAFARI 2000.

[38] The excellent agreement between τ_{is} and τ_{sp} obtained in the present study may be due in part to the fact that the aerosol in SAFARI 2000 was dominated by small, relatively nonhygroscopic, biomass burning aerosols, which are easier to sample than hygroscopic and/or larger particles such as mineral dust or sea salt.

4. Summary

[39] In this paper we have presented airborne in situ measurements of the vertical profiles of the ambient aerosol light scattering coefficient (σ_{sp}), dry aerosol absorption coefficient (σ_{apd}), aerosol single scattering albedo (ω_0), temperature and RH at a number of locations in Southern Africa during the dry, biomass burning season (August and September 2000). These measurements show large fluctuations in σ_{sp} and ω_0 with height in the boundary layer, due to the presence of haze layers and clean air slots, and a sharp decrease in σ_{sp} in passing from the boundary layer into the free troposphere (see Figures 2–8). The measurements also reflect the effects of local sources of biomass burning and of the long-range transport of biomass smoke. For example, prior to the intrusion of heavy smoke from the north (the "River of Smoke") into the region of measurements, the mean value of ω_0 was 0.89 ± 0.03, whereas, during the "River of Smoke" the mean value of ω_0 was 0.81 ± 0.02. The effects of long-range transport of biomass smoke, from the interior of southern Africa, on vertical profiles of aerosol optical properties on the Namibian coast have also been documented.

[40] Column AODs measured from close to the ground by a Sun photometer aboard the aircraft ranged from about 0.13 to 1.07. Comparisons of layer AODs from the Sun photometer with those derived from the in situ measurements of σ_{spd}, σ_{apd} and the humidification factor for light scattering (f_s), show excellent agreement (see Figure 17).

[41] **Acknowledgments.** We thank Raymond Weiss and Philip Russell for help in obtaining measurements. Funding for the University of Washington was provided by grants NAG5-9022 and NAG5-7675 from NASA's Radiation Science Program and grant ATM-9901624 from NSF's Division of Atmospheric Sciences. Funding for NASA Ames was provided by the NASA EOS-IDS and TOMS Programs under program codes 291-01-91-45, 622-44-75-10, and 621-14-01-00. This study is part of the SAFARI 2000 Southern African Regional Science Initiative.

References

Bodhaine, B. A., Aerosol absorption measurements at Barrow, Mauna Loa and the South Pole, *J. Geophys. Res.*, *100*, 8967–8975, 1995.

Bond, T. C., T. L. Anderson, and D. Campbell, Calibration and intercomparison of filter-based measurements of visible light absorption by aerosols, *Aerosol Sci. Technol.*, *30*, 582–600, 1999.

Eatough, D. J., D. A. Eatough, L. Lewis, and E. A. Lewis, Fine particulate chemical composition and light extinction at Canyonlands National Park using organic particulate material concentration obtained with a multisystem, multichannel diffusion denuder sampler, *J. Geophys. Res.*, *101*, 19,515–19,531, 1996.

Halthore, R. N., S. Nemesure, S. E. Schwartz, D. G. Imre, A. Berk, E. G. Dutton, and M. H. Bergin, Models overestimate diffuse clear-sky surface irradiance: A case for excess atmospheric absorption, *Geophys. Res. Lett.*, *25*, 3591–3594, 1998.

Hartley, S. W., P. V. Hobbs, J. L. Ross, P. B. Russell, and J. M. Livingston, Properties of aerosols aloft relevant to direct radiative forcing off the mid-Atlantic coast of the United States, *J. Geophys. Res.*, *105*, 9859–9885, 2000.

Hegg, D. A., J. Livingston, P. V. Hobbs, T. Novakov, and P. Russell, Chemical apportionment of aerosol optical depth off the mid-Atlantic coast of the United States, *J. Geophys. Res.*, *102*, 25,293–25,303, 1997.

Hobbs, P. V., Clean air slots amid atmospheric pollution, *Nature*, *415*, 861, 2002.

Hobbs, P. V., Clean air slots amid dense atmospheric pollution in southern Africa, *J. Geophys. Res.*, *108*(D13), 8490, doi:10.1029/2002JD002156, 2003.

Intergovernmental Panel on Climate Change (IPCC), *Climate Change 2001: The Scientific Basis*, edited by J. T. Houghton et al., 896 pp., Cambridge Univ. Press, New York, 2001.

Kato, S., M. H. Bergin, N. Laulainen, R. Ferrare, D. Turner, J. Michalsky, T. P. Charlock, E. E. Clothiaux, G. G. Mace, and T. P. Ackerman, A comparison of the aerosol optical thickness derived from ground-based and airborne measurements, *J. Geophys. Res.*, *105*, 14,701–14,717, 2000.

Magi, B. I., and P. V. Hobbs, Effects of humidity on aerosols in southern Africa during the biomass burning season, *J. Geophys. Res.*, *108*(D13), 8495, doi:10.1029/2002JD002144, 2003.

Redemann, J., P. B. Russell, and P. Hamill, Dependence of aerosol light absorption and single-scattering albedo on ambient relative humidity for sulfate aerosols with black carbon cores, *J. Geophys. Res.*, *106*, 27,485–27,495, 2001.

Remer, L. A., S. Gassó, D. A. Hegg, Y. J. Kaufman, and B. N. Holben, Urban/industrial aerosol: Ground-based Sun/sky radiometer and airborne in situ measurements, *J. Geophys. Res.*, *102*, 16,849–16,859, 1997.

Schmid, B., et al., Clear sky closure studies of lower tropospheric aerosol and water vapor during ACE 2 using airborne sunphotometer, airborne in-situ, space-borne, and ground-based measurements, *Tellus*, *B52*, 568–593, 2000.

Schmid, B., et al., Coordinated airborne, spaceborne, and ground-based measurements of massive thick aerosol layers during the dry season in southern Africa, *J. Geophys. Res.*, *108*(D13), 8496, doi:10.1029/2002JD002297, 2003.

Seinfeld, J. H., and S. N. Pandis, *Atmospheric Chemistry and Physics: From Air Pollution to Climate Change*, 1326 pp., John Wiley, New York, 1998.

Sinha, P., P. V. Hobbs, R. J. Yokelson, I. T. Bertschi, D. R. Blake, I. J. Simpson, S. Gao, T. W. Kirschstetter, and T. Novakov, Emissions of trace gases and particles from savanna fires in southern Africa, *J. Geophys. Res.*, *108*(D13), 8487, doi:10.1029/2002JD002325, 2003.

Swap, R. J., H. J. Annegarn, J. T. Suttles, M. D. King, S. Platnik, J. L. Privette, and R. J. Scholes, Africa burning: A thematic analysis of the Southern African Regional Science Initiative (SAFARI 2002), *J. Geophys. Res.*, *108*, doi:10.1029/2003JD003747, in press, 2003.

P. V. Hobbs and B. I. Magi, Department of Atmospheric Sciences, University of Washington, Box 351640, Seattle, WA 98195-1640, USA. (phobbs@atmos.washington.edu; magi@atmos.washington.edu)

J. Redemann and B. Schmid, Bay Area Environmental Research Institute, 645 Anthony Court, Sonoma, CA 95476, USA. (jredemann@mail.arc.nasa.gov; bschmid@mail.arc.nasa.gov)